

Severe osmotic compression triggers a slowdown of intracellular signaling, which can be explained by molecular crowding

Agnès Miermont^a, François Waharte^b, Shiqiong Hu^c, Megan Nicole McClean^d, Samuel Bottani^a, Sébastien Léon^e, and Pascal Hersen^{a,c,1}

^aLaboratoire Matière et Systèmes Complexes, Unité Mixte de Recherche (UMR) 7057, Centre National de la Recherche Scientifique (CNRS), Université Paris Diderot, 75013 Paris, France; ^bBiolmaging Cell and Tissue Core Facility (PICT-IBISA), UMR 144, CNRS, Institut Curie, 75005 Paris, France; ^cMechanobiology Institute, National University of Singapore, Singapore 117411; ^dLewis-Sigler Institute for Integrative Genomics, Princeton University, Princeton, NJ 08544; and ^eInstitut Jacques Monod, CNRS, Université Paris Diderot, 75013 Paris, France

Edited by David A. Weitz, Harvard University, Cambridge, MA, and approved February 15, 2013 (received for review September 4, 2012)

Regulation of the cellular volume is fundamental for cell survival and function. Deviations from equilibrium trigger dedicated signaling and transcriptional responses that mediate water homeostasis and volume recovery. Cells are densely packed with proteins, and molecular crowding may play an important role in cellular processes. Indeed, increasing molecular crowding has been shown to modify the kinetics of biochemical reactions in vitro; however, the effects of molecular crowding in living cells are mostly unexplored. Here, we report that, in yeast, a sudden reduction in cellular volume, induced by severe osmotic stress, slows down the dynamics of several signaling cascades, including the stress-response pathways required for osmotic adaptation. We show that increasing osmotic compression decreases protein mobility and can eventually lead to a dramatic stalling of several unrelated signaling and cellular processes. The rate of these cellular processes decreased exponentially with protein density when approaching stalling osmotic compression. This suggests that, under compression, the cytoplasm behaves as a soft colloid undergoing a glass transition. Our results shed light on the physical mechanisms that force cells to cope with volume fluctuations to maintain an optimal protein density compatible with cellular functions.

biophysics | HOG pathway | protein diffusion

The evolutionary adaptations of cells and organisms to specific environments are well characterized. Physiological adaptations to environmental variations are also important for cell survival and growth. Environmental challenges such as changes in temperature, pH, and osmolarity are known to alter cellular function. For example, temperature variations impact protein folding, the kinetics of biochemical reactions, and protein-binding specificities (1). The balance of water activity is a critical requirement for a wide range of cellular functions (2–5). On the one hand, a shift to a lower osmotic environment increases cell volume, threatening the integrity of the cellular membrane (4, 6, 7). To counteract such stress, bacteria and yeast are surrounded by highly resistant cell walls that mechanically protect them from bursting (4). On the other hand, high osmolarity causes water efflux and cell shrinkage (4, 8). In yeast, osmotic shrinkage is completed within a few tens of seconds after exposure to increased osmolarity (9). The final cell volume is set by the mechanical equilibration of external, internal, and turgor pressures (10, 11). Hyperosmotic stress alters a variety of cellular processes, such as disrupting the cytoskeleton structure (12, 13), inducing chromatin remodeling (14, 15), and triggering cell cycle arrest (16, 17) and apoptosis (18, 19). The high-osmolarity glycerol (HOG) pathway of the budding yeast *Saccharomyces cerevisiae* (Fig. 1A) orchestrates adaptation (20) to hyperosmotic shock to ensure water homeostasis and volume recovery, notably through glycerol production (4, 21). Several studies have provided a comprehensive, quantitative understanding of the dynamics of the HOG pathway (9–11, 20, 22–25). Membrane sensors (Sln1p, Msb2p, Hkr1p) are activated by osmotic stress and induce

successive phosphorylation of the HOG mitogen-activated protein kinases (MAPKs), culminating in dual phosphorylation of the Hog1p kinase (4) and leading to the Nmd5p-dependent nuclear import of Hog1p, which accumulates in the nucleus (Fig. 1A) and orchestrates a large transcriptional response.

One of the main physiological changes that occurs immediately after hyperosmotic stress is an increase in the intracellular protein concentrations and the total protein density, thus leading to molecular crowding. This may alter the mobility, folding, stability, and association rates of several proteins inside the cell. Molecular crowding has received little attention in living cells, although it is usually invoked to explain why biochemical reactions rates may vary in vivo and in vitro (26–29). For instance, the diffusion coefficient of the green fluorescent protein is typically 10 times lower in cells than in vitro (30).

Cells are densely packed with proteins. An estimate in yeast gives a typical protein density of a few hundred grams per liter for a volume fraction of typically 20–30%. Osmotically compressed cells will be even more crowded. However, the effects of increasing molecular crowding on cell signaling have not been experimentally investigated and are difficult to predict (1, 26, 28). Increasing the protein concentration increases the probability of protein interactions and protein association rates and may lead to more rapid biochemical kinetics. However, the diffusion of proteins may be reduced in an overcrowded cytoplasm (31, 32), thus slowing down biochemical kinetics.

Changing the cell volume by altering the osmotic pressure is a simple strategy to study the effect of increasing molecular crowding on active processes in living cells. Such strategy can be conveniently applied to yeast, and the HOG pathway is a natural candidate for study. The HOG pathway has been extensively studied in response to gentle and mild osmotic stresses (<1 M sorbitol). In such cases, the stronger the osmotic stimulation, the more potent and longer the duration of Hog1p nuclear localization (4, 11, 20, 24). A preliminary hint of what happens under more severe osmotic stresses, and thus stronger compression, came from a study by Van Wuytswinkel et al., who reported that Hog1p nuclear import and phosphorylation were surprisingly delayed under severe osmotic stress (1.4 M NaCl) (33); however, no satisfying explanation was given for this observation. Delayed nuclear import

Author contributions: A.M., S.L., and P.H. designed research; A.M., F.W., and S.H. performed research; S.H., M.N.M., S.B., S.L., and P.H. contributed new reagents/analytic tools; A.M., F.W., M.N.M., S.B., S.L., and P.H. analyzed data; and A.M. and P.H. wrote the paper.

The authors declare no conflict of interest.

This article is a PNAS Direct Submission.

Freely available online through the PNAS open access option.

¹To whom correspondence should be addressed. E-mail: pascal.hersen@univ-paris-diderot.fr.

This article contains supporting information online at www.pnas.org/lookup/suppl/doi:10.1073/pnas.1215367110/-DCSupplemental.

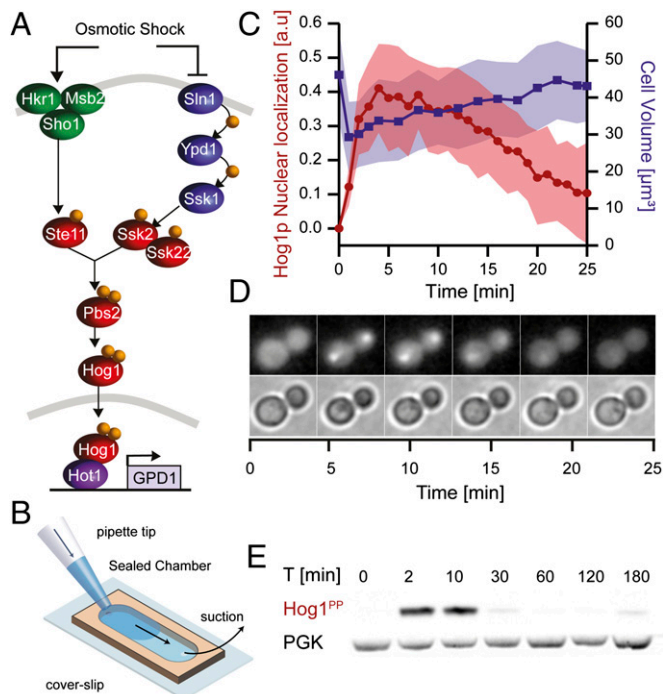


Fig. 1. Dynamics of the HOG cascade. (A) HOG cascade. (B) Illustration of the sealed gasket chambers used to experimentally regulate the cells' environment. (C) Osmotic stimulation (1 M sorbitol) induced immediate cell shrinkage (blue curve) followed by nuclear accumulation of Hog1p (red curve). Data are represented as the mean of several cells \pm 1 SD ($n > 20$). Cells progressively recovered their size and switched off the HOG cascade through negative-feedback loops. (D) Nuclear accumulation of Hog1p was rapid and robust after a 1 M sorbitol osmotic stress. (E) Phosphorylation levels of Hog1p after a 1 M sorbitol osmotic stress followed the same pattern with a rapid induction and then a slow decay. Typically, within 30 min, nuclear Hog1p was no longer observed, and Hog1p returned to basal phosphorylation levels. Phosphoglycerate kinase (PGK) was used as a positive control.

and phosphorylation of Hog1p under severe osmotic stress could be attributable to a loss of the activity of a sensor or a kinase, a decrease in the nucleocytoplasmic transport of Hog1p, salt toxicity, or, alternatively, the effects of molecular crowding attributable to osmotic compression, as discussed above. In this article, we set out to address the effects of osmotic compression on signaling dynamics by monitoring several signaling processes in yeast over a range of osmotic stresses.

Results

Both Phosphorylation and Nuclear Import of Hog1p Are Slowed Down During Severe Osmotic Compression. To study the dynamics of activation of the HOG cascade, we measured changes in the nuclear fluorescence of Hog1p-GFP yeast cells immobilized in a sealed gasket chamber (Fig. 1B). The environment of the cells was rapidly changed (typically in less than 10 s; Fig. S1) from normal yeast media to the same media supplemented with sorbitol. After 1 M sorbitol treatment, Hog1p became phosphorylated and was imported into the nucleus within a few minutes (Fig. 1C–E). The cell volume immediately decreased after osmotic stimulation with 1 M sorbitol and then restored progressively over time (Fig. 1C). The dynamics of Hog1p nuclear translocation and phosphorylation under these conditions were very reproducible and in agreement with the literature (9, 23).

We then studied the behavior of the HOG pathway in response to stronger osmotic stresses (Fig. 2). Both the time taken to observe Hog1p phosphorylation and the time needed to reach maximal Hog1p nuclear localization increased when osmotic compression

increased (Fig. 2). Under gentle stimulation (1 M sorbitol), the maximum nuclear intensity was reached after \sim 2–3 min, whereas for severe shock (\sim 1.8 M sorbitol), maximum nuclear intensity was reached after \sim 55 min (Fig. 2B and F and Movie S1). Thus, increasing the sorbitol concentration from 1 M to 1.8 M reduced the nuclear import rate of Hog1p by one order of magnitude. Similar results were obtained when using NaCl as an osmotic agent (Fig. S2). As the sorbitol concentration increased, the rate of Hog1p phosphorylation also reduced (Fig. 2D) and correlated well with the time taken for nuclear localization of Hog1p to be observed (Fig. 2E and F). Note that Hog1p nuclear translocation was synchronously observed for all cells subjected to osmotic shock lower than 1.8 M sorbitol. However, the proportion of cells that displayed nuclear enrichment of Hog1p quickly decreased when the intensity of osmotic stress increased above 1.8 M sorbitol (Fig. S2). When exposed to 2 M sorbitol, only 25% of the cells displayed nuclear localization of Hog1p, even after several hours of observation; this effect was not related to cell death, because most cells remained viable even after several hours of osmotic treatment (Fig. S3).

Timing of Hog1p Nuclear Import Is Correlated with the Decrease in Cell Volume. Cell volume decreased with increasing osmotic stress, reaching a plateau at around 40% of the initial cell volume for sorbitol concentrations above \sim 2 M (Fig. 2C). This is in

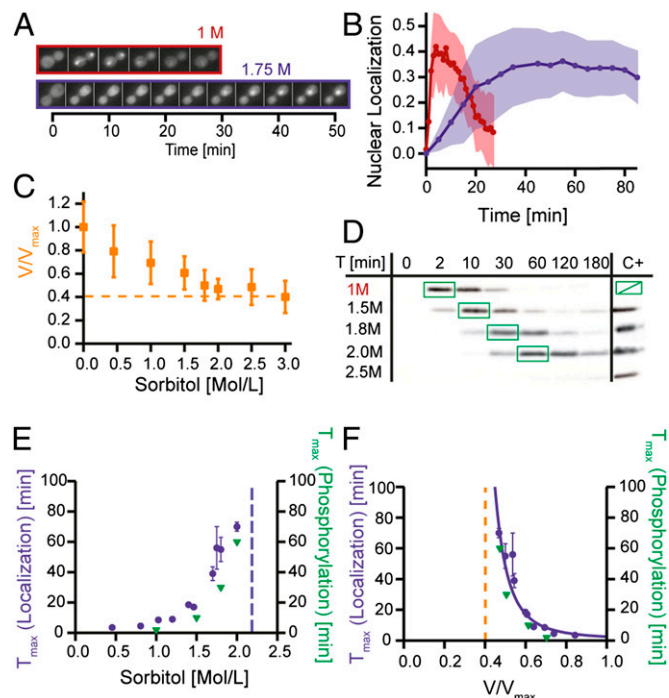


Fig. 2. Severe osmotic stress reduces the kinetics of HOG activation and nuclear translocation. (A) Time-lapse imaging of the nuclear localization of Hog1p in cells exposed to 1 M (red) and 1.75 M (blue) sorbitol. (B) The rate of Hog1p nuclear translocation was reduced by severe osmotic shock (red, 1 M sorbitol; blue, 1.75 M sorbitol). Maximal nuclear accumulation was observed \sim 45–60 min after 1.75 M sorbitol treatment (E). (C) Cell volume decreased with increasing concentrations of sorbitol, down to a plateau at around \sim 40% of the initial volume. (D) Western blots showing Hog1p phosphorylation over time and under increasing osmotic stress. Phosphorylation of Hog1p after 2 min at 1 M sorbitol is used as a positive control (C+). (E) Time at which the Hog1p nuclear concentration and phosphorylation levels reached a maximum increased with the strength of the osmotic shock. Above 2.2 M sorbitol (blue dashed), no cells displayed nuclear accumulation of Hog1p (Fig. S2). (F) Same data as in E, shown as a function of relative cell volume compression. The blue line is a fit consistent with what is expected for a soft colloid near a glassy transition, $T = T_0 \frac{V}{V_{\text{max}}} e^{\alpha V_{\text{max}}/V}$, where $T_0 = 0.065$ and $\alpha = 3.6$.

agreement with Schaber et al., who proposed the minimum compression volume for yeast cells to be between 33% and 49% of their normal volume (10). The delays in both Hog1p phosphorylation and nuclear translocation correlated with the changes in cell volume: the smaller the cell volume (measured immediately after osmotic stress), the slower the dynamics of Hog1p phosphorylation and nuclear translocation (Fig. 2*F*). More precisely, the timing of Hog1p activation displayed a divergent behavior when the cell volume approached $V/V_{\max} \approx 0.4$ (Discussion and Fig. S4).

Diffusion of Hog1p Reduces in Osmotically Compressed Cells. We conducted fluorescence recovery after photobleaching (FRAP) experiments to investigate whether the reduced rate of Hog1p translocation in a crowded cytoplasm could be explained by a decrease in protein mobility. We used *HOG1-GFP pbs2Δ* cells (Fig. 3 and Movie S2). In a *pbs2Δ* background, the HOG pathway is genetically disrupted, and Hog1p-GFP cannot be phosphorylated or imported into the nucleus. FRAP experiments can thus be performed in any osmotic environment without triggering nuclear enrichment of Hog1p-GFP. We observed that the diffusion of Hog1p-GFP (Fig. 3 and Movie S2) decreased with increasing osmotic compression. Fluorescence recovery took less than a second in isotonic conditions, and around 5 s after a gentle osmotic stress (1 M sorbitol; Fig. S5). We obtained a diffusion coefficient of $\sim 15 \mu\text{m}^2\cdot\text{s}^{-1}$ in isotonic conditions and $\sim 1.7 \mu\text{m}^2\cdot\text{s}^{-1}$ after stress with 1 M sorbitol (Fig. S5). However, no recovery after photobleaching was observed after treatment with 2 M sorbitol (Fig. 3*A*), and it was not possible to quantify the diffusion coefficient. Fluorescence loss in photobleaching (FLIP) experiments (Fig. 3*D* and *E*, Fig. S6, and Movie S2) confirmed this result: cells continuously bleached at the same location entirely lost their fluorescence in isotonic conditions, but not after a sudden, severe osmotic stress. Similar results were obtained when using other fluorescently tagged proteins in a wild-type background (Fig. S6). These results are also in good agreement with previous measurements of the effect of molecular crowding on

diffusion (28, 31, 32) and indicate that severe osmotic compression decreases the mobility of Hog1p.

Nuclear Translocation of Msn2p Is also Delayed During Severe Hyperosmotic Compression. To further test whether the observed slowdowns in nuclear translocation, phosphorylation and protein mobility were specific to components of the HOG pathway, we examined the dynamics of the nuclear translocation of Msn2p (34–36), a key transcription factor in the general stress response of yeast. After hyperosmotic stress, Msn2p is hyperphosphorylated and imported into the nucleus (37). Nuclear import of Msn2p is achieved via a different mechanism to Hog1p; Msn2p contains a nuclear localization signal and does not interact a priori with Nmd5p (36). We nevertheless observed the same scenario as for Hog1p: the rate of nuclear translocation of Msn2p progressively reduced as osmotic compression increased (Fig. 4*A* and *E* and Movie S3); this effect was not dependent on alterations to the dynamics of Hog1p, as a similar behavior was observed in a *hog1Δ* background (Fig. S7).

Dynamics of the Nuclear Translocation of Yap1p, Crz1p, and Mig1p Are Delayed When Cells Are Osmotically Compressed. We further tested the nuclear-translocation dynamics of transcription factors that are not specifically activated by osmotic stress: Yap1p, Crz1p, and Mig1p (Fig. 4 and Movies S4, S5, and S6). Yap1p is involved in the oxidative stress response and contains a nuclear localization signal but is constantly exported from the nucleus by Crm1p (38). The addition of 300 μM hydrogen peroxide (H_2O_2) triggers oxidation of the cysteine residues in Yap1p, leading to a conformational change that blocks its nuclear export by Crm1p. Hence, Yap1p accumulates in the nucleus upon oxidative stress. The transcription factor Crz1p is a cytoplasmic protein involved in the regulation of calcium ion homeostasis. Upon stimulation with calcium, Crz1p is dephosphorylated and imported into the nucleus (39). In the presence of glucose, Mig1p is dephosphorylated by the Reg1p-Glc7p protein phosphatase complex and imported into the nucleus, where it binds to the promoters of glucose-repressed genes (40).

In the following experiments, the objective was to reduce the cell volume using severe hyperosmotic shock and, simultaneously, to activate and measure the nuclear translocation of these transcription factors. We applied a dual input of a severe hyperosmotic shock and a stimulus of either 300 μM H_2O_2 (Yap1p), 200 mM Ca^{2+} (Crz1p), or 2% (wt/wt) glucose, which were added to cells initially grown in galactose (Mig1p). In isotonic conditions, Crz1p localized to the nucleus within a few minutes of the addition of Ca^{2+} (Fig. 4*B*). This burst of nuclear translocation was delayed by several minutes when the cells were stimulated with Ca^{2+} in combination with severe hyperosmotic shock (1.4 M sorbitol; Fig. 4*B* and *F*). Interestingly, Crz1p was also partially activated to undergo nuclear translocation by mild osmotic stress alone (Fig. 4*B*); this effect may be attributable to variations in the internal calcium concentration following cell shrinkage. Note that when stimulated by a severe hyperosmotic stress alone, the dynamics of Crz1p nuclear translocation was also slowed down, in agreement with our hypothesis that increasing osmotic compression reduces the rate of intracellular signaling (Fig. 4*B*). Similarly, we observed a marked reduction in the rate of nuclear import of Yap1p (Fig. 4*C* and *G*) and Mig1p (Fig. 4*D* and *H*) when the cells were both stimulated and osmotically compressed; these slowdowns became more pronounced with increasing volumetric compression (Fig. 4*J* and Fig. S4). Taken together, these results suggest that a nonspecific slowdown in the kinetics of nuclear translocation occurs when cellular volume is reduced through a severe osmotic compression.

Dynamics of Endocytosis and Vesicular Trafficking Are Reduced During Osmotic Shock. To gain further insight into the effect of osmotic compression, we investigated the effects of osmotic compression on the dynamics of three additional processes. We

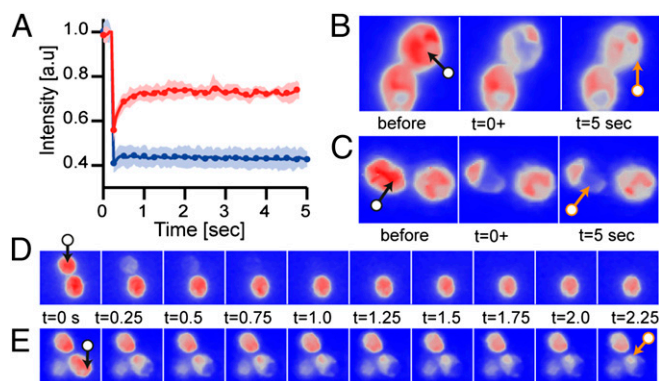


Fig. 3. Diffusion of Hog1p-GFP in the cytoplasm is decreased by osmotic compression. (A) FRAP experiments on the *HOG1-GFP pbs2Δ* strain in SC medium (red curve) and after 2 M sorbitol stress (blue curve). (B) FRAP images of *HOG1-GFP pbs2Δ* cells in SC medium before bleaching (Left), immediately after bleaching (Center), and 5 s later (Right). The bleached area is indicated by the black arrow, and its recovery is indicated by the orange arrow. (C) FRAP images of a *HOG1-GFP pbs2Δ* cell in a severe osmotic environment (2 M sorbitol). In contrast to B, the bleached area did not recover after 5 s. (D) FLIP time series for a *HOG1-GFP pbs2Δ* cell in SC medium. The same spot was continuously bleached (black arrow), and total cell fluorescence rapidly decreased compared with the unbleached neighboring cell. (E) After severe osmotic compression, the cell maintained some cytoplasmic fluorescence over a long time (orange arrow), indicating that the diffusion of fluorescent protein was very limited. Pictures are color-coded to improve visualization (blue for low intensity and red for high intensity).

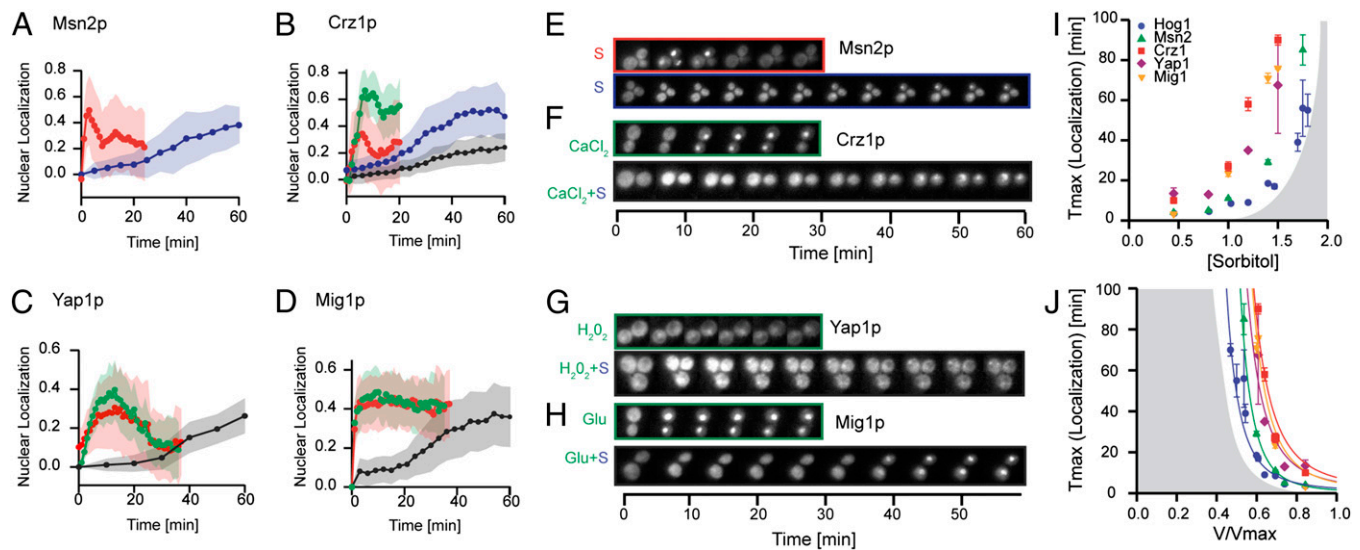


Fig. 4. Several signaling cascades are delayed when the cell volume is suddenly decreased by osmotic compression. (A) Nuclear localization of Msn2p in response to gentle osmotic stress (0.45 M sorbitol, red) and severe osmotic stress (1.75 M sorbitol, blue). (B) Nuclear localization of Crz1p in response to calcium shock (200 mM, green), gentle osmotic stress (0.45 M sorbitol, red), severe osmotic stress (1.75 M sorbitol, blue), and combined calcium shock and severe volume reduction by osmotic stress (200 mM Ca^{2+} plus 1.4 M sorbitol, black). (C) Nuclear localization of Yap1p in response to oxidative stress (300 μM H_2O_2 , green), oxidative stress and gentle osmotic compression (300 μM H_2O_2 plus 0.45 M sorbitol, red), and combined oxidative stress and severe osmotic stress (H_2O_2 plus 1.4 M sorbitol, black). (D) Nuclear localization of Mig1p in response to glucose (20 g/L, green), combined glucose and gentle osmotic stress (glucose plus 0.45 M sorbitol, red), and combined glucose and severe osmotic stress (glucose plus 1.4 M sorbitol, black). Cells were precultured in galactose without glucose. For A–D, data are represented as the mean of many cells ($n > 20$) \pm 1 SD. (E–H) Time-lapse images of the nuclear localization of Msn2p (E), Yap1p (F), Crz1p (G), and Mig1p (H). “S” indicates sorbitol, and the concentrations used and color code are the same as for A–D. (I and J) Measurement of the time to reach maximum nuclear localization of Msn2p (sorbitol), Yap1p (H_2O_2), Crz1p (Ca^{2+}), Mig1p (glucose), and Hog1p (sorbitol) as a function of either the additional sorbitol concentration used (I) or the relative cell volume (J). The curves fit the function $T = T_0 \frac{V}{V_{\text{max}}} e^{\alpha V_{\text{max}}/V}$ that models the behavior of a soft colloid. For Msn2p, $T_0 = 0.035$ and $\alpha = 3.9$; for Crz1p, $T_0 = 0.096$ and $\alpha = 4.4$; for Yap1p, $T_0 = 0.077$ and $\alpha = 4.3$; for Mig1p, $T_0 = 0.043$ and $\alpha = 4.8$.

first analyzed the mobility of the protein Abp1p, an actin-binding protein that dynamically partitions between the plasma membrane and endosomes under normal conditions (41). After sudden and severe osmotic stress (3 M sorbitol), Abp1p patches suddenly stopped their random motion (Fig. S8 and Movie S7). We also examined Sec7p, which is involved in protein transport and is found in the cytoplasm and Golgi-associated coated vesicles (42). The mobility of Sec7p was drastically impaired by osmotic compression (Fig. S8 and Movie S8). Finally, using a tracer of bulk endocytosis, the fluorescent dye FM4-64 (43), we observed that the active internalization and transport of vesicles stalled after sudden osmotic compression (Fig. S8).

Signaling Dynamics Quickly Recover When Cell Volume Is Restored. If the reductions observed in the dynamics of cell signaling were only attributable to a reduction in cell volume, the cells should be able to recover their normal signaling activity upon the restoration of cell volume. Hence, we investigated signaling dynamics after the recovery of cell volume, as illustrated in Fig. 5A. Hog1p-GFP or Msn2p-GFP cells were subjected to a severe osmotic stress and then returned to a less hyperosmotic environment, to relax the osmotic compression (Fig. 5B and C). We did not return the cells to isotonic conditions, because we wanted to determine whether Hog1p and Msn2p translocated to the nucleus, which does not happen in isotonic conditions. Whereas cells did not show any nuclear localization during the first 5 min of severe osmotic stress, marked, rapid localization of Hog1p and Msn2p became visible when the cells were returned to a less hyperosmotic environment (1 M sorbitol). Thus, the cells were still alive and could function properly as soon as the osmotic clamp was mechanically relaxed. Similar experiments were performed for Crz1p, Mig1p, and Yap1p (Fig. 5D–F). Initially, in the presence of severe osmotic stress, the cells did not display any localization activity for any of these pathways. However, relaxation of the osmotic constraint led to the rapid

activation of these pathways. Therefore, although decreasing the cell volume inhibited the signal-processing ability of the cells, their signal-processing ability was recovered as soon as the cell volume was restored.

Discussion

Taken together, our experiments demonstrate that severe osmotic compression drastically reduces the rate of several dynamic processes in living cells. Reducing the volume of yeast cells led to a lower diffusion coefficient and slower rates of Hog1p phosphorylation and nuclear import. The dynamics of the nuclear translocation of other transcription factors (Yap1p, Crz1p, Msn2p, and Mig1p) were similarly delayed by osmotic compression. Importantly, release of the osmotic clamp on the cells led to a rapid recovery of signaling. Each of the proteins tested is activated by a different process (phosphorylation, dephosphorylation, and oxidation) and undergoes nuclear import via a different mechanism, and yet the kinetics of their nuclear translocation displayed a similar dependence on osmotic compression. In addition, the kinetics of actin-binding protein mobility, vesicular trafficking, and endocytosis were also reduced by osmotic compression. These observations argue in favor of a general, nonspecific, physical slowdown process.

The cytoplasm is a dense assembly of proteins in a liquid, namely a colloid. Interestingly, when a colloid becomes too dense, its relaxation dynamics are dramatically slowed down, and its viscosity increases dramatically. Similarly, if the cytoplasm becomes too crowded, it becomes very difficult for proteins to diffuse, and their mobility drastically reduces. Zhou et al. (44) recently demonstrated that higher eukaryotic cells behave as soft colloids: colloids made of deformable particles. During the glassy transition of soft colloids, the viscosity diverges exponentially with the colloid volume fraction, ϕ (45). Assuming that the diffusion coefficient of a protein, D , scales as the inverse of the cytoplasmic viscosity, and that the rates of diffusion limited reactions scale with ϕD , the

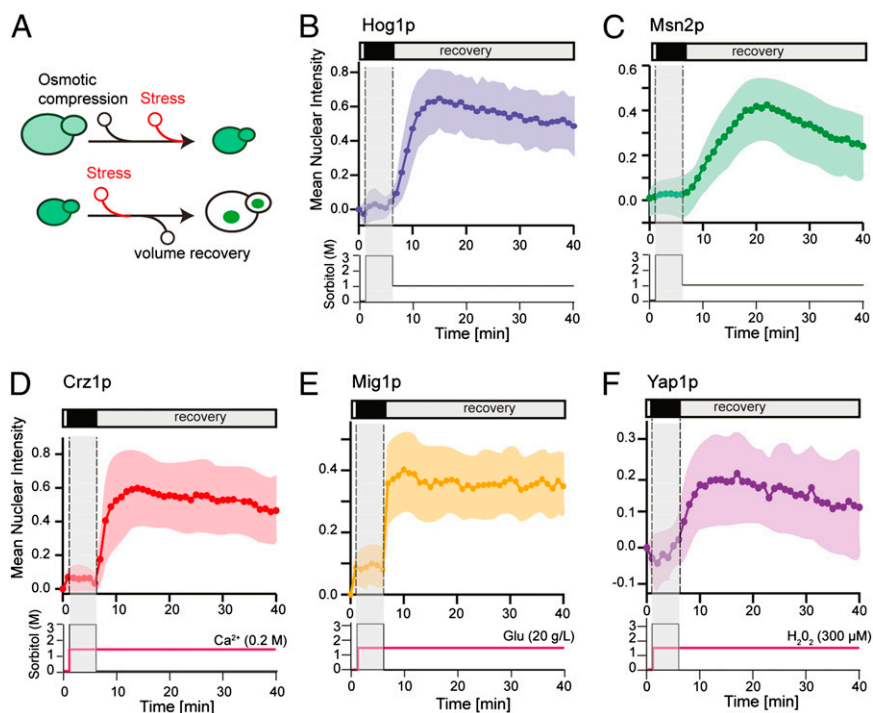


Fig. 5. Signaling-cascade dynamics are immediately restored upon recovery of the cell volume. (A) Principle of signaling activation by volume recovery. Cells are stressed and, at the same time, osmotically compressed by severe osmotic stress (3 M sorbitol). The osmotic compression was then relaxed by a return to a lower osmotic stress conditions, and we investigated whether the cells could detect and respond to the chemical stress that was still present in the cells' environment. (B–F) Time courses of the nuclear localization of Hog1p (B), Msn2p (C), Crz1p (D), Mig1p (E), and Yap1p (F) under these experimental conditions. As soon as the volume of the cell was restored, the studied signaling cascades could function normally, as indicated by nuclear localization of their respective transcription factors.

typical timescale of a diffusion limited reaction should scale as $e^{c\phi}/\phi$. This scaling is in good agreement with our measurements (see the fitting curve in Figs. 2F and 4J and Fig. S4). This suggests that osmotically compressed yeast cells behave as soft colloids and undergo a glassy transition under too-severe compression. This also supports our hypothesis that osmotic compression leads to a decrease in the mobility of proteins in the cytoplasm, because of an increase in molecular crowding. Our results emphasize the importance of molecular crowding, induced by hyperosmotic compression in our experiments, in determining the kinetics of biochemical reactions within cells.

Recently, Dill et al. (1) outlined that cellular function should be analyzed within the context of the mechanical and thermodynamic constraints exerted by the environment. Dill et al. argued that an optimal protein density must exist, which originates from the competition between the two counteracting effects discussed at the beginning of this article: increasing molecular crowding enhances the rate of biochemical reactions but only up to the point where the negative effects of molecular crowding on protein diffusion become dominant. Our results in living cells support this view. We hypothesize that the size of cells was determined by evolution, so that cells usually function at a protein density that enables them to resist mild and sudden changes in osmolarity. Thus, the total protein density is likely to be smaller than the optimum proposed by Dill et al., because cells with too high of a protein density would be at risk for the complete arrest of key cellular processes upon sudden osmotic shock: a behavior obviously not favored by evolution. Our results outline why the protein density, or the cell volume, must be regulated in order for cells to function properly. We propose that the effects of molecular crowding should be taken into account when considering the biological (gene networks, signaling) and physical (cellular mechanics) properties that constrain cellular dynamics.

Materials and Methods

Yeast Strains and Maintenance. Cultures were maintained in YPD medium [1% yeast extract (Difco; 0127-17), 2% Bacto Peptone (Difco; 0118-17), 2% glucose (VWR; 24379.294)] or in Synthetic Complete (SC) medium (0.67% yeast nitrogen base without amino acids; Fisher; W1706W), 2% glucose (VWR; 24379.294), and 0.08% Complete Supplement Mixture dropout mixture (MP Biomedicals; 114500012). Cells were grown overnight at 30 °C in SC, reinoculated into fresh SC, and grown at 30 °C for 4–6 h before microscopy. See Tables S1 and S2 for details on the yeast strains. Details on the preparation of protein extracts and Western blotting are given in SI Materials and Methods.

Sudden Osmotic Stimulation. Perfusion chamber gaskets from Invitrogen (4 chambers, 19 mm × 6 mm, 80 μ L; C-18128) were used as an inexpensive and simple system to switch the cells from one environment to another. A solution of Con A (2 mg/mL; MP Biomedicals; 2150710.2) was added into the chamber, and, after 15 min of incubation, yeast cells were injected and allowed 10–15 min to adhere to the coverslip before starting the experiment.

Microscopy and Image Analysis. The cells were observed using an Olympus IX81 inverted fluorescent microscope with a QuantEM 5125C camera and a 100 \times /1.40 NA immersion oil objective. GFP emission was visualized at 528 nm (38-nm bandwidth) upon excitation at 490 nm (20-nm bandwidth); mCherry was visualized at 617 nm (73-nm bandwidth) upon excitation at 555 nm (28-nm bandwidth). Images were acquired using MetaMorph software (Molecular Devices), and image analysis was performed with ImageJ (46). The fluorescence intensity of transcription factors in the nucleus was obtained by measuring the intensity of GFP colocalized with the nuclear marker Htb2p-mCherry. We removed the background from the GFP channel (rolling ball method with a radius of 200 pixels), applied a Gaussian blur (1 pixel) to reduce noise, found a threshold to separate the cells from the background (Otsu thresholding), and segmented the cells using the “analyze particles” and “watershed” plugins of ImageJ. We computed the relative nuclear intensity as $[GFP(\text{nucleus}) - GFP(\text{cytoplasm})]/GFP(\text{cytoplasm})$ and renormalized all cells by subtracting the value for first measurement performed before osmotic compression. The area of the cell was measured by fitting ellipses to the contour of the cells. From the cell area, we computed the equivalent cell volume assuming that cells are spheres with

a radius $r = (\text{area}/\pi)^{1/2}$. We measured the relative volume for each cell using V/V_{max} in which V_{max} is the volume of the cell before osmotic compression.

FRAP and FLIP Experiments. FRAP and FLIP experiments were performed at the Nikon Imaging Centre of the Institut Curie. Experiments were performed at 30 °C on a total internal reflection fluorescence Nikon Eclipse Ti inverted fluorescent microscope equipped with a QuantEM 512SC camera, and a 100× 1.45 NA immersion oil objective. The emission filter wavelength was 525 nm, and the excitation filter was 470 nm. For bleaching, we used a 491-nm pulse generated by a FRAP 4D module (Roper). A cytoplasmic area of typically 2 μm in diameter was photo-bleached by a 50-ms laser pulse. A single focal plane was then recorded every 50 ms with a 50-ms exposure time. FLIP experiments were performed using the same system; however, the images were recorded every 250 ms. FRAP images were denoised using the ND-Safir software on 10 cells for each condition. This procedure, developed by Boulanger et al.

(47), improves the signal to noise ratio and is crucial for the quantitative analysis of FRAP data. Once denoised, the images were normalized by the fluorescence intensity of the bleached area just before the bleach. Additional FRAP experiments were performed using a spinning disk microscope at the Mechanobiology Institute of Singapore (Fig. S6 C, D, F, and G).

ACKNOWLEDGMENTS. We thank J. Uhlendorf, G. Batt, G. Charvin, S. Rutherford, C. Dargemont, and J.-M. Di Meglio for insightful discussions on and critical reading of the manuscript. We also thank J. Salamero for advice on the “FRAP 4D module” and the FRAP/FLIP experiments, and the Nikon Imaging Center of the Institut Curie. A.M. is a student of the Frontiers of Living Systems doctoral program. We acknowledge the support of the Agence Nationale de la Recherche (DISIP-ANR-07-JCJC-0001 and ICEBERG-ANR-10-BINF-06-01), the C’Nano(ModEnv) program, the “Who am I?” Laboratory of Excellence (ANR-11-LABX-0071 and ANR-11-IDEX-0005-01), the Mechanobiology Institute, and the Laboratoire International Associé Cell Adhesion France-Singapour (CAFS).

- Dill KA, Ghosh K, Schmit JD (2011) Physical limits of cells and proteomes. *Proc Natl Acad Sci USA* 108(44):17876–17882.
- Strange K (2004) Cellular volume homeostasis. *Adv Physiol Educ* 28(1-4):155–159.
- Ho SN (2006) Intracellular water homeostasis and the mammalian cellular osmotic stress response. *J Cell Physiol* 206(1):9–15.
- Hohmann S (2002) Osmotic stress signaling and osmoadaptation in yeasts. *Microbiol Mol Biol Rev* 66(2):300–372.
- Hüssinger D (1996) The role of cellular hydration in the regulation of cell function. *Biochem J* 313(Pt 3):697–710.
- Grant WD (2004) Life at low water activity. *Philos Trans R Soc Lond B Biol Sci* 359(1448):1249–1266.
- Lang F, et al. (1998) Functional significance of cell volume regulatory mechanisms. *Physiol Rev* 78(1):247–306.
- Petelenz-Kurdiel E, et al. (2011) Quantification of cell volume changes upon hyperosmotic stress in *Saccharomyces cerevisiae*. *Integr Biol (Camb)* 3(11):1120–1126.
- Hersen P, McClean MN, Mahadevan L, Ramanathan S (2008) Signal processing by the HOG MAP kinase pathway. *Proc Natl Acad Sci USA* 105(20):7165–7170.
- Schaber J, et al. (2010) Biophysical properties of *Saccharomyces cerevisiae* and their relationship with HOG pathway activation. *Eur Biophys J* 39(11):1547–1556.
- Klipp E, Nordlander B, Krüger R, Gennemark P, Hohmann S (2005) Integrative model of the response of yeast to osmotic shock. *Nat Biotechnol* 23(8):975–982.
- Chowdhury S, Smith KW, Gustin MC (1992) Osmotic stress and the yeast cytoskeleton: Phenotype-specific suppression of an actin mutation. *J Cell Biol* 118(3):561–571.
- Slaninová I, Sesták S, Svoboda A, Farkas V (2000) Cell wall and cytoskeleton reorganization as the response to hyperosmotic shock in *Saccharomyces cerevisiae*. *Arch Microbiol* 173(4):245–252.
- Kültz D, Chakravarty D (2001) Maintenance of genomic integrity in mammalian kidney cells exposed to hyperosmotic stress. *Comp Biochem Physiol A Mol Integr Physiol* 130(3):421–428.
- Mas G, et al. (2009) Recruitment of a chromatin remodelling complex by the Hog1 MAP kinase to stress genes. *EMBO J* 28(4):326–336.
- Escoté X, Zapater M, Clotet J, Posas F (2004) Hog1 mediates cell-cycle arrest in G1 phase by the dual targeting of Sic1. *Nat Cell Biol* 6(10):997–1002.
- Clotet J, et al. (2006) Phosphorylation of Hsl1 by Hog1 leads to a G2 arrest essential for cell survival at high osmolarity. *EMBO J* 25(11):2338–2346.
- Silva RD, et al. (2005) Hyperosmotic stress induces metacaspase- and mitochondria-dependent apoptosis in *Saccharomyces cerevisiae*. *Mol Microbiol* 58(3):824–834.
- Galvez A, et al. (2001) A rapid and strong apoptotic process is triggered by hyperosmotic stress in cultured rat cardiac myocytes. *Cell Tissue Res* 304(2):279–285.
- Muzzey D, Gómez-Urbe CA, Mettetal JT, van Oudenaarden A (2009) A systems-level analysis of perfect adaptation in yeast osmoregulation. *Cell* 138(1):160–171.
- Miermont A, Uhlendorf J, McClean MN, Hersen P (2011) The Dynamical Systems Properties of the HOG Signaling Cascade. *J Signal Transduct* 2011:930940.
- O’Rourke SM, Herskowitz I (2004) Unique and redundant roles for HOG MAPK pathway components as revealed by whole-genome expression analysis. *Mol Biol Cell* 15(2):532–542.
- Mettetal JT, Muzzey D, Gómez-Urbe C, van Oudenaarden A (2008) The frequency dependence of osmo-adaptation in *Saccharomyces cerevisiae*. *Science* 319(5862):482–484.
- Zi Z, Liebermeister W, Klipp E (2010) A quantitative study of the Hog1 MAPK response to fluctuating osmotic stress in *Saccharomyces cerevisiae*. *PLoS ONE* 5(3):e9522.
- Pelet S, et al. (2011) Transient activation of the HOG MAPK pathway regulates bimodal gene expression. *Science* 332(6030):732–735.
- Minton AP (2001) The influence of macromolecular crowding and macromolecular confinement on biochemical reactions in physiological media. *J Biol Chem* 276(14):10577–10580.
- Ellis RJ (2001) Macromolecular crowding: Obvious but underappreciated. *Trends Biochem Sci* 26(10):597–604.
- Zhou H-X, Rivas G, Minton AP (2008) Macromolecular crowding and confinement: Biochemical, biophysical, and potential physiological consequences. *Annu Rev Biophys* 37:375–397.
- Schoen I, Kramer H, Braun D (2009) Hybridization kinetics is different inside cells. *Proc Natl Acad Sci USA* 106(51):21649–21654.
- Konopka MC, Shkel IA, Cayley S, Record MT, Weisshaar JC (2006) Crowding and confinement effects on protein diffusion in vivo. *J Bacteriol* 188(17):6115–6123.
- Dorsaz N, De Michele C, Piazza F, De Los Rios P, Foffi G (2010) Diffusion-limited reactions in crowded environments. *Phys Rev Lett* 105(12):120601.
- Roosen-Runge F, et al. (2011) Protein self-diffusion in crowded solutions. *Proc Natl Acad Sci USA* 108(29):11815–11820.
- Van Wuytswinkel O, et al. (2000) Response of *Saccharomyces cerevisiae* to severe osmotic stress: Evidence for a novel activation mechanism of the HOG MAP kinase pathway. *Mol Microbiol* 37(2):382–397.
- Garreau H, et al. (2000) Hyperphosphorylation of Msn2p and Msn4p in response to heat shock and the diauxic shift is inhibited by cAMP in *Saccharomyces cerevisiae*. *Microbiology* 146(Pt 9):2113–2120.
- Beck T, Hall MN (1999) The TOR signalling pathway controls nuclear localization of nutrient-regulated transcription factors. *Nature* 402(6762):689–692.
- Görner W, et al. (1998) Nuclear localization of the C2H2 zinc finger protein Msn2p is regulated by stress and protein kinase A activity. *Genes Dev* 12(4):586–597.
- Capaldi AP, et al. (2008) Structure and function of a transcriptional network activated by the MAPK Hog1. *Nat Genet* 40(11):1300–1306.
- Delaunay A, Isnard AD, Toledano MB (2000) H2O2 sensing through oxidation of the Yap1 transcription factor. *EMBO J* 19(19):5157–5166.
- Polizotto RS, Cyert MS (2001) Calcineurin-dependent nuclear import of the transcription factor Crz1p requires Nmd5p. *J Cell Biol* 154(5):951–960.
- Nehlin JO, Carlberg M, Ronne H (1991) Control of yeast GAL genes by MIG1 repressor: A transcriptional cascade in the glucose response. *EMBO J* 10(11):3373–3377.
- Kaksonen M, Sun Y, Drubin DG (2003) A pathway for association of receptors, adaptors, and actin during endocytic internalization. *Cell* 115(4):475–487.
- Franzusoff A, Redding K, Crosby J, Fuller RS, Schekman R (1991) Localization of components involved in protein transport and processing through the yeast Golgi apparatus. *J Cell Biol* 112(1):27–37.
- Vida TA, Emr SD (1995) A new vital stain for visualizing vacuolar membrane dynamics and endocytosis in yeast. *J Cell Biol* 128(5):779–792.
- Zhou EH, et al. (2009) Universal behavior of the osmotically compressed cell and its analogy to the colloidal glass transition. *Proc Natl Acad Sci USA* 106(26):10632–10637.
- Mattsson J, et al. (2009) Soft colloids make strong glasses. *Nature* 462(7269):83–86.
- Rasband WS (1997–2012) ImageJ (National Institutes of Health, Bethesda). Available at <http://imagej.nih.gov/ij/>. Accessed December 18, 2012.
- Boulanger J, et al. (2010) Patch-based nonlocal functional for denoising fluorescence microscopy image sequences. *IEEE Trans Med Imaging* 29(2):442–454.

Supporting Information

Miermont et al. 10.1073/pnas.1215367110

SI Materials and Methods

For western blotting and protein extract, cells were grown in appropriate synthetic medium to $OD_{600} = 1$. They were collected by filtration and then stressed with different sorbitol concentrations (1–2.5 M) for the indicated time period. To prepare protein extracts, cultures were rapidly suspended in 10% trichloroacetic acid (Sigma; T0699) and maintained in ice for at least 10 min. Cells were centrifuged, and maximum supernatant was discarded to leave around 100 μL in the tubes. Cells were broken by bead-beating the samples (10 min at 4 $^{\circ}\text{C}$) with glass beads (425–600 μm) (Sigma; G8772). The samples were centrifuged, the supernatant was discarded, and the pellet was resuspended in SDS buffer (1 \times NuPage buffer, 10% β mercaptoethanol, and 200 mM Tris) to a final volume of 100 μL . Samples were loaded on 10% SDS/PAGE NuPage

precast gel (Invitrogen; NP0315BOX) in 1 \times NuPage running buffer (Invitrogen; NP0001) and run at 180 V for 1 h. Proteins were transferred to PVDF membranes (Invitrogen; LC2005) at 30 V at 4 $^{\circ}\text{C}$ overnight. Dual phosphorylation of Hog1p on Thr-174 and Tyr-176 was examined in a Western blot analysis using an anti-dually phosphorylated p38 antibody 1:1,000 (Cell Signaling Technologies; 9211L), and the positive control was examined using phosphoglycerate kinase monoclonal primary antibody 1:1,000 (Invitrogen; 22C5D8). Goat anti-rabbit-HRP secondary antibodies (Jackson ImmunoResearch; 111-035-003) were used at a dilution of 1:10,000. Antibody binding was visualized using ECL-plus system (Amersham; GE RPN2132) in a Fujifilm LAS 4000 imaging system. Membranes were stripped between both primary antibodies using 62.5 mM Tris-HCl (pH 6.8) with 2% SDS.

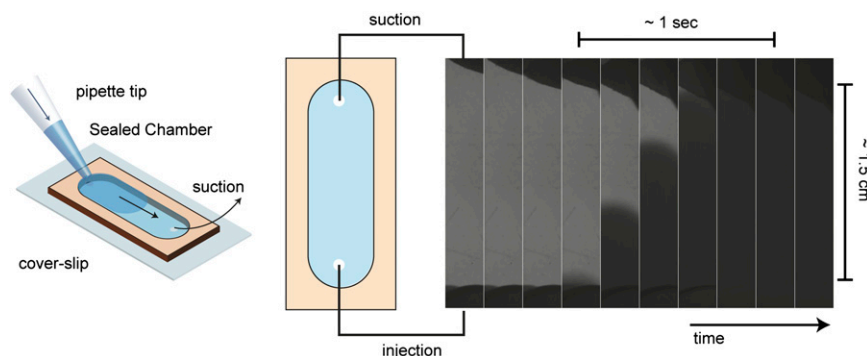


Fig. S1. Quick exchange of fluids in a gasket sealed chamber. Using a pipette at one inlet of the gasket and a paper filter (black area at the top) at the outlet to generate a flow, it is possible to replace the entire volume of liquid contained in the chamber within a few seconds. The actual time it takes to replace water (light gray) with a liquid containing a dye (seen as a dark gray area rising vertically) is of the order of 1 s (there is 0.2 s between each images). A few additional seconds are required to get the pipette and the filter correctly aligned with the inlet and outlet of the gasket chamber. In practice, one needs typically 10 s to complete this operation.

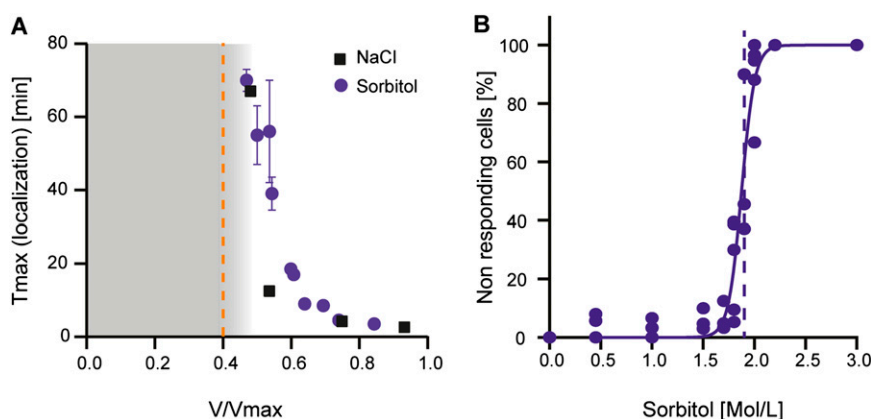


Fig. S2. Additional data regarding Hog1p slowdown by osmotic compression. (A) Both NaCl and sorbitol triggered similar slowdown of the HOG cascade when plotted as a function of the relative cell volume variation. (B) For mild osmotic stresses (<1.5 M sorbitol), all cells eventually displayed a Hog1p nuclear localization. However, there was an abrupt transition around 2 M sorbitol, above which almost no cells displayed Hog1p nuclear translocation, even after more than 2 h of observation. Fitting the data with a sigmoid gave a transition at around 1.9 M sorbitol, for which 50% of the cells were not responsive.

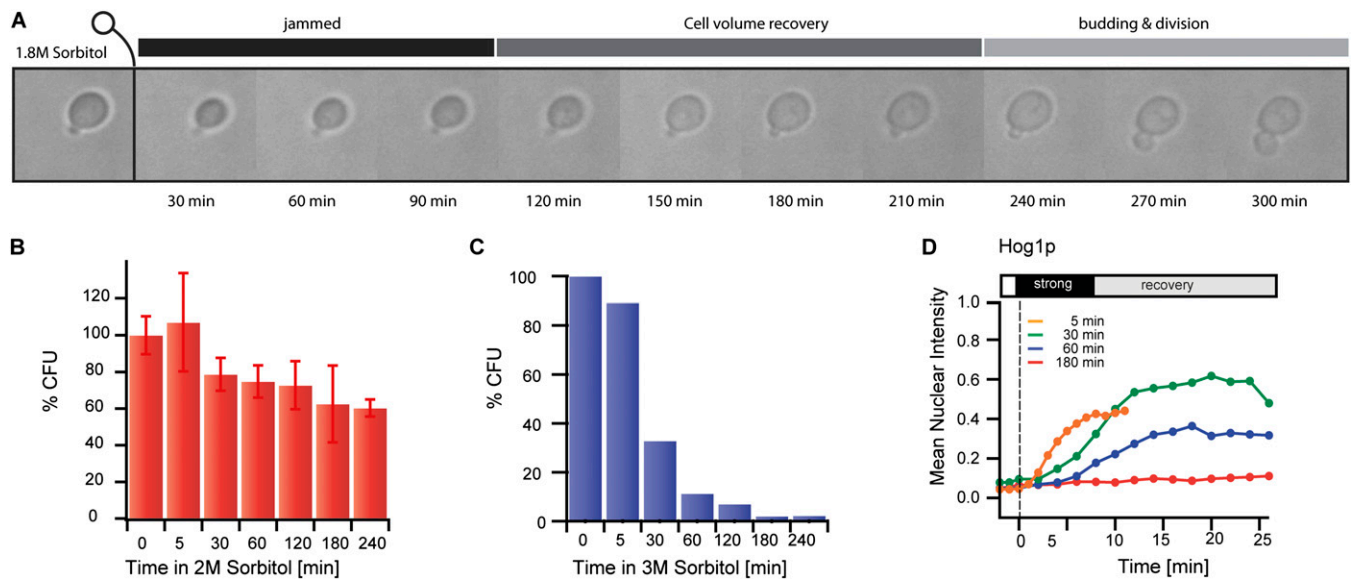


Fig. 53. Prolonged exposure to severe osmotic stress. (A) Cells can adapt to severe osmotic stress. Upon 1.8 M sorbitol stress, cells appear jammed at first. It took several hours for cells to eventually adapt and divide. We did not image cells for longer than ~4 h (the medium has to be changed very regularly to avoid artifacts caused by evaporation), and, thus, we did not observe cell adaptation and recovery for 2 M sorbitol shocks. However, cells can survive and adapt to such strong shocks as shown by colony-forming unit experiments. (B and C) We counted the number of colony-forming units on plates that were seeded after different periods of exposure to 2 or 3 M sorbitol. In both cases, short exposure (5 min) resulted in a high survival rate. For long exposure to 2 M sorbitol stress, the survival rate was of the order of 50%. (C) The survival rate was much lower in the case of very severe 3 M sorbitol shock. (D) Therefore, we were careful not to let the cells stay for too long in 3 M sorbitol when we performed the experiments of volume compression and recovery shown in Fig. 4. To illustrate its short-term effect on cell signaling, we applied a very severe stress (3 M sorbitol) for increasing periods of time (from 5 min to 3 h) before changing the environment back to yeast synthetic medium supplemented with 1 M sorbitol. The average dynamics of nuclear translocation of Hog1-GFP was slower and slower even if the proportion of responding cells was larger than 90% for stress shorter than 1 h. After a too-long exposition to 3 M sorbitol (>1 h), cells were unable to recover and only very few cells showed some localization (~15%). It is tempting to hypothesize that the progressive loss of efficiency in Hog1p dynamics and cell death after a too-long exposure are attributable to the arrest of internal maintenance and homeostatic processes when cells are severely osmotically compressed.

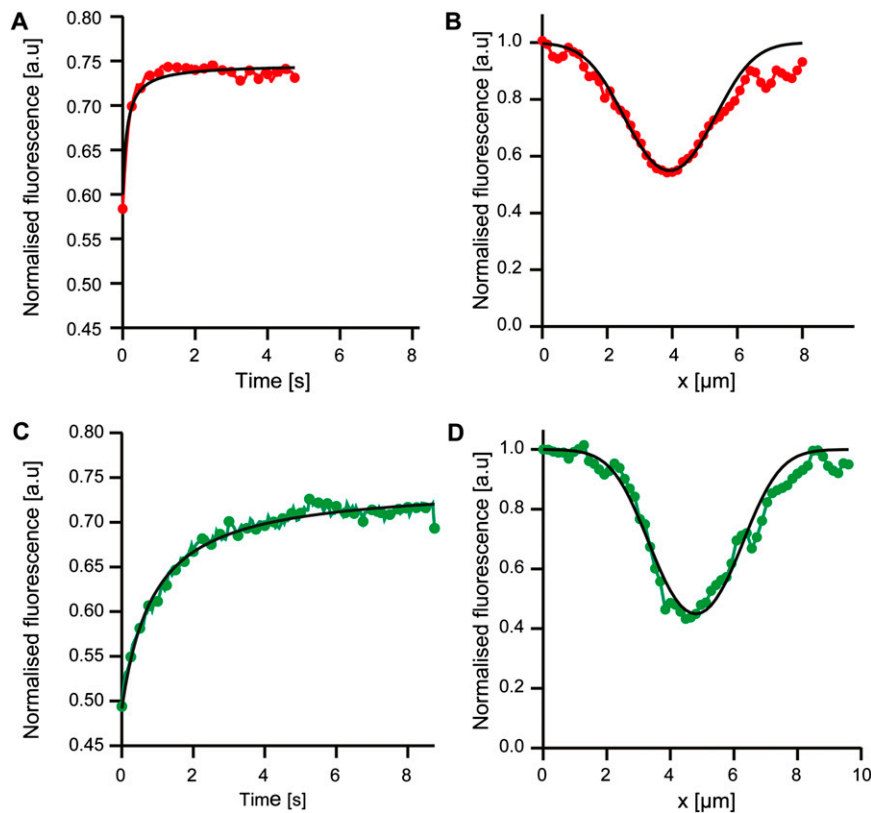


Fig. S5. Fluorescence recovery after photobleaching of Hog1p-GFP; *pbs2Δ* cells. (A and B) Fluorescence recovery after photobleaching (FRAP) experiments performed in Synthetic Complete (SC) medium. (A) Average profile of fluorescence recovery over six cells. (B) Transverse section of the averaged photobleached area for one cell, illustrating the size of the bleached area. (C and D) Same results but for 10 cells stimulated by a gentle osmotic shock (SC supplemented with 1 M sorbitol). Note that in both conditions, the size of the bleached area is large enough ($\sim 1.8 \mu\text{m}$ theoretically, $\sim 2.4 \mu\text{m}$ in practice) to prevent fluorescence recovery to the initial fluorescence value [1 in arbitrary unit (a.u.)]. It is then difficult to estimate with precision a diffusion coefficient. To estimate the diffusion coefficient, we first extracted the average Gaussian bleached fluorescent profile. Then we determined the characteristic time of diffusion (τ) from fluorescence recovery curves (Fig. 3 and Fig. S3). The coefficient of diffusion, D , was then estimated by taking into account that particles will diffuse over the bleached area radius, w_m , in the typical time τ with a diffusion coefficient $D = w_m^2/4\tau$. From the FRAP data made in normal growth conditions (SC medium; Fig. 3 and Fig. S5), we obtained $\tau = 0.091 \text{ s}$, $w_m = 2.4 \mu\text{m}$, and, thus, $D = 15.8 \mu\text{m}^2\cdot\text{s}^{-1}$. From the FRAP data made in SC supplemented with 1 M sorbitol, we found $\tau = 0.85 \text{ s}$, $w_m = 2.4 \mu\text{m}$, and, thus, $D = 1.7 \mu\text{m}^2\cdot\text{s}^{-1}$. We were not able to measure it for severe osmotic stress because diffusion was apparently stalled (Fig. 3 and Fig. S6).

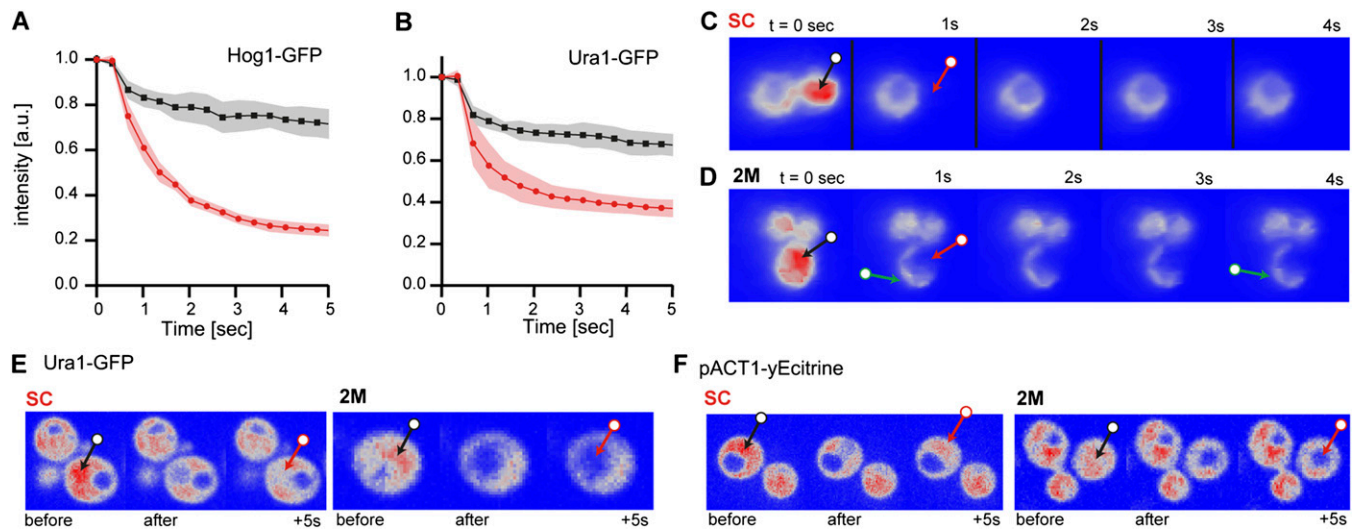


Fig. S6. Additional FRAP/fluorescence loss in photobleaching (FLIP) experiments. (A) FLIP data corresponding to the images shown in Fig. 3C for a Hog1-GFP, *pbs2Δ* background. Whereas the fluorescence is quickly lost outside of the continuously bleached spot (red curve) in isotonic conditions, some fluorescence remains visible outside of the bleached spot when the cell is osmotically stressed with 2 M sorbitol (black curve; see also Fig. 3). (B) FLIP data acquired on the fluorescent protein Ura1p-GFP (isotonic conditions, red; 2 M sorbitol stress, black). Severe osmotic stress led to a drastically reduced protein mobility (see also E). (C and D) Image time series of a FLIP experiment using a URA1-GFP strain. Note the green arrows that show that a residual fluorescence can be seen outside of the bleached area after a severe osmotic stress but not in isotonic conditions. (E and F) FRAP experiments using the Ura1p-GFP protein and the fluorescent protein yEctrine constitutively expressed. The difference of dynamics between isotonic and hyperosmotic conditions is obvious. Images are taken before, immediately after, and 5 s after the bleach. The arrows show the approximate location of the bleach. Whereas the bleached spot recovers (partially) its fluorescence in isotonic conditions, there is no recovery of fluorescence for strongly osmotically compressed cells, and the bleached, dark spot remains as if fluorescent proteins were “frozen.” This again shows that there is a drastic loss of protein mobility in osmotically compressed cells.

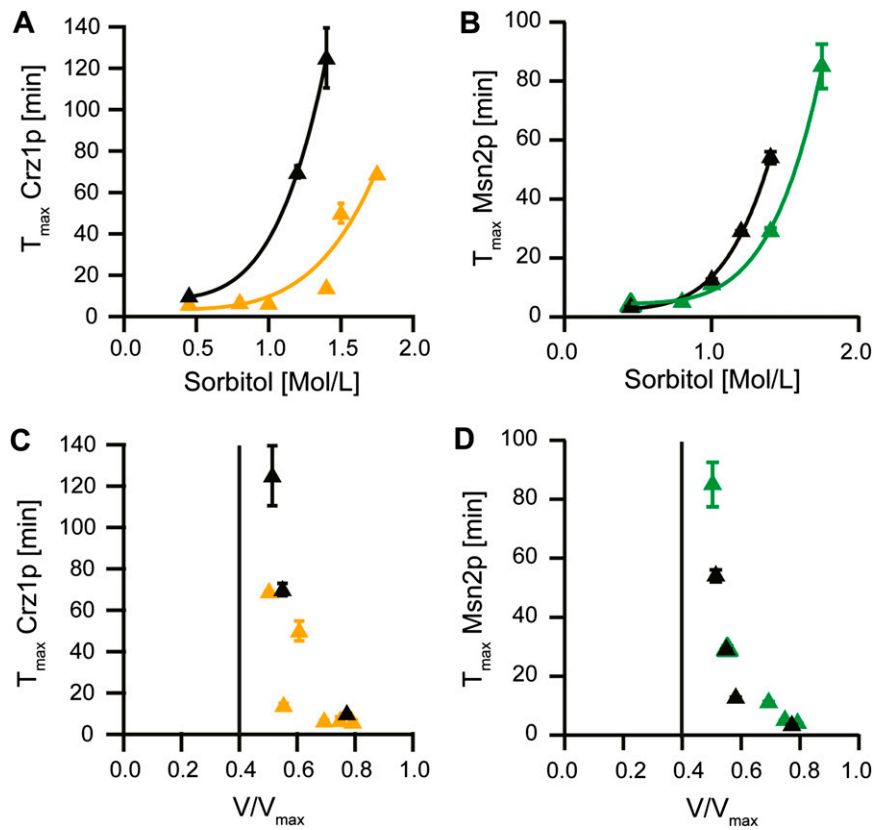


Fig. S7. Crz1p and Msn2p dynamics in a *hog1Δ* background. (A) We measured Crz1p nuclear-translocation dynamics in a *hog1Δ* strain (black) and compared it to a *HOG1* strain (yellow). (B) We also compared Msn2p nuclear-translocation dynamics in a *hog1Δ* strain (black) and in a *HOG1* strain (green). Both experiments showed that the slowdown is more pronounced in a *hog1Δ* strain when studied as a function of the sorbitol concentration. Because Hog1p is a key regulator of cell size regulation and cell wall integrity, it is likely that in a *hog1Δ* strain, a difference in turgor, internal osmolarity, cell wall composition, or initial cell size may be responsible for a different osmotic compressibility. Importantly, the *hog1Δ* mutant appears to behave as a *HOG1* strain when plotted in function of the volume variation (C and D). This is in agreement with our findings that pointed out the relevance of volume compression: the absolute value of the osmotic stress is not relevant here.

Table S1. List of relevant strains used in this study

Name	Background	Genotype	Source
yPH015	BY4742	<i>HOG1-GFP-HIS3 HTB2-mCherry-URA3</i>	Hersen et al. (1)
yPH016	yPH15	<i>HOG1-GFP-HIS3 HTB2-mCherry-URA3 pbs2Δ-Kan</i>	Hersen et al. (1)
yPH033	BY4741	<i>MSN2-GFP-HIS3MX6 HTB2-mCherry-KanMX4</i>	This study
yPH069	BY4741	<i>CRZ1-GFP-HIS3MX6 HTB2-mCherry-KanMX4</i>	This study
yPH107	BY4741	<i>MIG1-GFP-HIS3MX6 HTB2-mCherry-KanMX4</i>	This study
yPH082	BY4742	<i>YAP1-GFP-HIS3</i> + plasmid pRS316-mCherry	F. Devaux, Université Pierre et Marie Curie, Paris
yPH114	BY4741	<i>ABP1-GFP-HIS3</i>	S.L. laboratory
yPH115	BY4741	<i>SEC7-mCherry_KanMX4</i>	S.L. laboratory

1. Hersen P, McClean MN, Mahadevan L, Ramanathan S (2008) Signal processing by the HOG MAP kinase pathway. *Proc Natl Acad Sci USA* 105(20):7165–7170.

Table S2. List of relevant plasmids

Name	Genotype	Source
pRS316-mCherry	URA3 CEN6 ARSH4 <i>mCherry</i>	F. Devaux, Université Pierre et Marie Curie, Paris
pFA6-hphNT1	<i>hphNT1</i>	PCR-toolbox Collection (1) (EUROSCARF)
pYM35	<i>DsRed1 KanMX4</i>	PCR-Toolbox Collection (1) (EUROSCARF)
pFA6-HIS3MX6	<i>HIS3MX6</i> marker for gene deletion	EUROSCARF
pYM35-mCherry	C-terminal tagging with mCherry, <i>KanMX4</i> marker	S.L. laboratory

1. Janke C, et al. (2004) A versatile toolbox for PCR-based tagging of yeast genes: New fluorescent proteins, more markers and promoter substitution cassettes. *Yeast* 21(11):947–962.

Hog1-GFP Dynamics is slowed down by severe osmotic compression

Severe osmotic compression triggers a slow down of intracellular signaling which can be explained by molecular crowding

A. Miermont, F. Waharte, S. Hu, M.N. McClean, S. Bottani, S. Léon & P. Hersen*

✉ pascal.hersen@univ-paris-diderot.fr 🌐 <http://tinyurl.com/TeamHersen>

PARIS DIDEROT CITE

Movie S1. Hog1p activity in function of osmotic compression. Differential Hog1p-GFP nuclear translocation of yeast cells subjected to either 1 or 1.75 M sorbitol stress. The dynamics of translocation are slower in the case of a severe osmotic stress.

[Movie S1](#)

FRAP / FLIP Dynamics when cells are osmotically compressed.

Severe osmotic compression triggers a slow down of intracellular signaling which can be explained by molecular crowding

A. Miermont, F. Waharte, S. Hu, M.N. McClean, S. Bottani, S. Léon & P. Hersen*

✉ pascal.hersen@univ-paris-diderot.fr 🌐 <http://tinyurl.com/TeamHersen>

UNIVERSITÉ PARIS DIDEROT CITE

Movie S2. FRAP/FLIP in function of osmotic compression. FRAP/FLIP experiments on Hog1p-GFP in three osmotic environments of increasing osmolarity. Diffusion is progressively reduced. The red circles indicate the bleached area. The recovery is too fast to be seen in regular SC, whereas it remains visible at all times in 2 M sorbitol.

[Movie S2](#)

Msn2-GFP Dynamics is slowed down by severe osmotic compression

Severe osmotic compression triggers a slow down of intracellular signaling which can be explained by molecular crowding

A. Miermont, F. Waharte, S. Hu, M.N. McClean, S. Bottani, S. Léon & P. Hersen*

✉ pascal.hersen@univ-paris-diderot.fr 🌐 <http://tinyurl.com/TeamHersen>

UNIVERSITÉ PARIS DIDEROT CITE

Movie S3. Msn2p activity in function of osmotic compression. Differential Msn2p-GFP nuclear translocation of yeast cells subjected to either 1 or 1.75 M sorbitol stress. The dynamics of translocation are slower in the case of a severe osmotic stress.

[Movie S3](#)

Crz1-GFP Dynamics is slowed down by severe osmotic compression

Severe osmotic compression triggers a slow down of intracellular signaling which can be explained by molecular crowding

A. Miermont, F. Waharte, S. Hu, M.N. McClean, S. Bottani, S. Léon & P. Hersen*

✉ pascal.hersen@univ-paris-diderot.fr 🌐 <http://tinyurl.com/TeamHersen>

UNIVERSITÉ PARIS DIDEROT CITE

Movie S4. Crz1p activity in function of osmotic compression. Differential Crz1p-GFP nuclear translocation of yeast cells stimulated with Ca^{2+} alone or together with an osmotic compression. The dynamics of translocation are slower in the case of a severe osmotic compression.

[Movie S4](#)

Yap1-GFP Dynamics is slowed down by severe osmotic compression

Severe osmotic compression triggers a slow down of intracellular signaling which can be explained by molecular crowding

A. Miermont, F. Waharte, S. Hu, M.N. McClean, S. Bottani, S. Léon & P. Hersen*

✉ pascal.hersen@univ-paris-diderot.fr 🌐 <http://tinyurl.com/TeamHersen>

UNIVERSITÉ PARIS DIDEROT CITE

Movie S5. Yap1p activity in function of osmotic compression. Differential Yap1p-GFP nuclear translocation of yeast cells stimulated with H_2O_2 alone or together with an osmotic compression. The dynamics of translocation are slower in the case of a severe of osmotic compression. Note that Yap1p-GFP does not show a very bright nuclear localization and photobleaches quickly.

[Movie S5](#)

Mig1-GFP Dynamics is slowed down by severe osmotic compression

Severe osmotic compression triggers a slow down of intracellular signaling which can be explained by molecular crowding

A. Miermont, F. Waharte, S. Hu, M.N. McClean, S. Bottani, S. Léon & P. Hersen*

✉ pascal.hersen@univ-paris-diderot.fr 🌐 <http://tinyurl.com/TeamHersen>

PARIS DIDEROT CITE

Movie S6. Mig1p activity in function of osmotic compression. Differential Mig1p-GFP nuclear translocation of yeast cells stimulated with glucose alone or together with an osmotic compression. The dynamics of translocation is slower in the case of a severe osmotic compression.

[Movie S6](#)

Abp1-GFP Dynamics after a severe osmotic compression

Severe osmotic compression triggers a slow down of intracellular signaling which can be explained by molecular crowding

A. Miermont, F. Waharte, S. Hu, M.N. McClean, S. Bottani, S. Léon & P. Hersen*

✉ pascal.hersen@univ-paris-diderot.fr 🌐 <http://tinyurl.com/TeamHersen>

PARIS DIDEROT CITE

Movie S7. Abp1p dynamics in function of osmotic compression. Abp1p-GFP dynamics in normal medium (SC) or after a severe osmotic compression, which drastically slows down Abp1p mobility in the cell.

[Movie S7](#)

Sec7-mCherry Dynamics after a severe osmotic compression

Severe osmotic compression triggers a slow down of intracellular signaling which can be explained by molecular crowding

A. Miermont, F. Waharte, S. Hu, M.N. McClean, S. Bottani, S. Léon & P. Hersen*

✉ pascal.hersen@univ-paris-diderot.fr 🌐 <http://tinyurl.com/TeamHersen>

UNIVERSITÉ PARIS DIDEROT CITE

Movie S8. Sec7p dynamics in function of osmotic compression. Sec7p-mCherry dynamics in normal medium (SC) or after a severe osmotic compression, which drastically slows down Sec7p mobility in the cell. The second part of the movie shows that for a 1.5 M sorbitol shock, Sec7p dynamics are restored after cells volume recovery.

[Movie S8](#)